

Miniaturisation in flow injection analysis

Practical limitations from a theoretical point of view

W. E. van der Linden
Enschede, The Netherlands

Introduction

Flow injection analysis (FIA) is a well established technique nowadays. One of the interesting features is its low reagent consumption in conjunction with the relatively small sample volumes required. This aspect will become even more important when a further reduction of the dimensions of the systems can be achieved. Technically such a miniaturisation does not present great problems as far as transport conduits or reaction compartments are concerned. Photolithographic techniques developed in chip-technology have reached a remarkable degree of perfection and offer excellent possibilities in this respect. A well known example is the miniature gas chromatograph etched on a silicon wafer of match box size as described by Angell *et al.*¹.

Some years ago Růžička and Hansen^{2,3} suggested a similar approach for flow injection manifolds. In their so-called 'integrated micro conduits' a large part of the manifold was manufactured by engraving grooves and other parts in a small single block of perspex, also of match box size. However, because of the mechanical engraving technique used, they did not actually reduce the size of the conduits and the major advantage of their design seems to be the diminution of the outer size together with the integration of the various component parts of a manifold in a permanent and rigid position. This contributes significantly to the enhanced repeatability that was experimentally observed. Since lithographic techniques offer the possibility of manufacturing manifolds with smaller dimensions, it is worthwhile to examine the possible problems arising from such a scaling-down. To facilitate further discussions some technological concepts will be introduced first.

Technological concepts

In chemical engineering scaling problems are generally discussed in terms of dimensionless numbers. These are characteristic entities composed of an ap-

propriate set of physical parameters in such a way that the resulting number can be interpreted as the ratio of two physical mechanisms or phenomena.

Well known is the Reynolds number (Re):

$$\text{Re} = \frac{2R\langle v \rangle \rho}{\eta} = 2 \frac{R\langle v \rangle}{\nu} \quad (1)$$

where R is the tube radius, $\langle v \rangle$ the mean linear velocity, ρ the density, η the dynamic and ν the kinematic viscosity. The Reynolds number can be interpreted as the ratio of momentum transport by convection and by internal friction. The value of about 2000 is rather crucial: at $\text{Re} < 2000$ the flow is laminar and a parabolic velocity profile is established (Fig. 1), whereas at $\text{Re} > 2000$ turbulence will prevail accompanied by a much flatter velocity profile.

Another dimensionless number that will be used is the Péclet number (Pe) which represents the ratio of mass transport by convection and by diffusion:

$$\text{Pe} = \frac{\langle v \rangle x}{D} \quad (2)$$

where x is a characteristic length and D is the diffusion coefficient. In the case of tubes two Péclet numbers can be distinguished, viz. the longitudinal Péclet number (Pe_L) where the characteristic length is equal to the tube length, and the radial Péclet

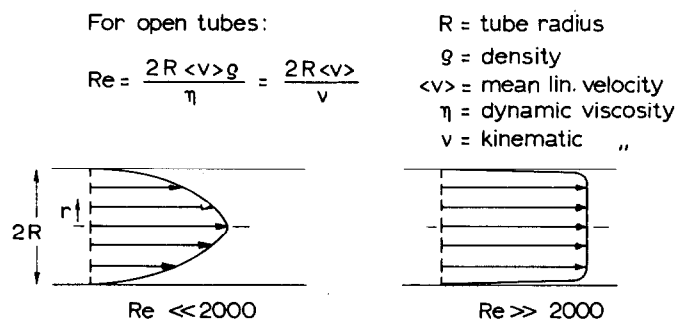


Fig. 1. Velocity profiles for two different values of the Reynolds number.

number (Pe_R) in which the characteristic length is equal to the tube diameter.

A third number, which provides the ratio of rates of momentum transport and mass transport, is the Schmidt number (Sc):

$$Sc = \frac{\nu}{D} \quad (3)$$

It should be noted that

$$Re \cdot Sc = \frac{2R\langle v \rangle}{\nu} \cdot \frac{\nu}{D} = \frac{2R\langle v \rangle}{D} \equiv Pe_R \quad (4)$$

Finally, a dimensionless number related to the residence time (t_v) is needed. Therefore a reduced time (τ) is introduced and defined as follows:

$$\tau = \frac{t_v D}{R^2} \quad (5)$$

After this small excursion in the domain of transport phenomena to get acquainted with some of the more important dimensionless numbers, the discussion of scaling in FIA can be continued.

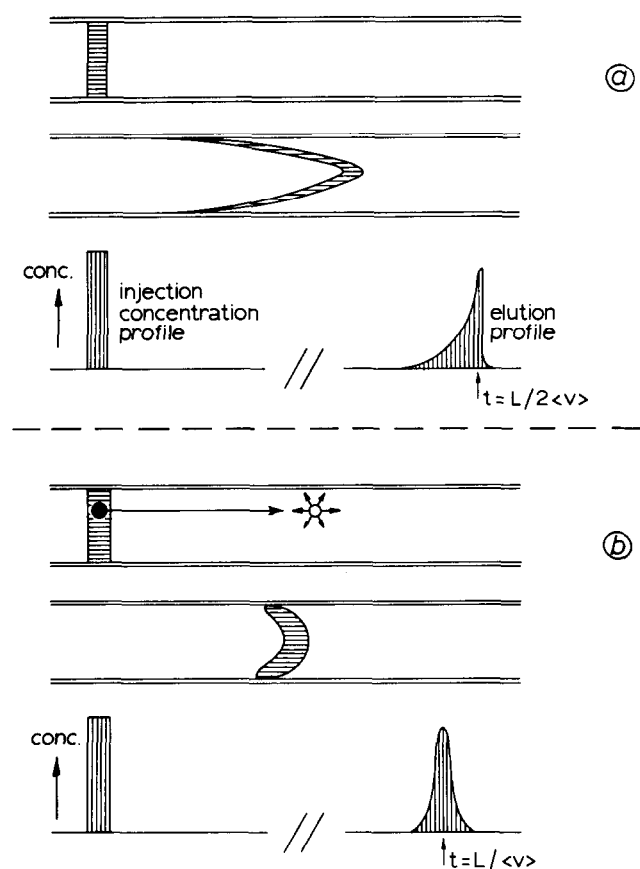


Fig. 2. Dispersion of sample plug and corresponding detector signal (a) without significant radial diffusion, and (b) with significant radial diffusion.

Application of technological concepts in FIA

A closer look at the process of sample plug transport by a carrier stream under ideal laminar flow conditions will reveal that an originally rectangular plug will adopt a parabolic shape according to the velocity profile of the fluid (Fig. 2a). The concentration profile observed by the detector will be asymmetric with a peak maximum at about $t = L/2\langle v \rangle$. In this figure the effect of diffusion has been neglected. If, however, the flow-rate is relatively low, diffusion will play a more important role. The radial component is of particular importance because it will cause the transport of molecules to other streamlines, *i.e.* to regions with different flow velocities. When the residence time is long enough each molecule will have an equal chance to remain for a certain period of time on each streamline, causing an averaging of the velocity of all molecules. This results in a reduced band broadening and in a detector signal that is more or less Gaussian-shaped (Fig. 2b). The maximum appears at $t = L/\langle v \rangle$. According to Taylor⁴, who was the first to give a quantitative description of this type of sample dispersion, the standard deviation of the peak can be presented by

$$\sigma_t = \sqrt{\frac{2D_L L}{\langle v \rangle^3}} \quad (6)$$

$$\text{where } D_L = \frac{R^2 \langle v \rangle^2}{48 D} \quad (7)$$

Combination of eqns. 6 and 7 with the condition $t_v = L/\langle v \rangle$ leads to

$$\sigma_t = \sqrt{\frac{t_v R^2}{24 D}} \quad (8)$$

Apart from minor differences, several authors have shown that at $\tau \geq 1$ Taylor-flow will prevail. More recently Aris has extended this description by taking into account the axial or longitudinal diffusion component.

Dispersion experiments can be characterized by their $Re \cdot Sc$ or Pe_R values in relation to the reduced time. In Fig. 3 the region of (Aris-)Taylor-flow is shown, and the region in which the majority of FIA determinations have to be located is indicated.

It is noteworthy that most determinations are performed outside the Taylor-region and, accordingly, tailing peaks are common practice. This also implies that apart from the small shaded band no mathematically useful description of the dispersion process is available. The shaded band indicates the region where rather complicated analytical results are obtained by Ananthakrishnan *et al.*⁵ For the region at

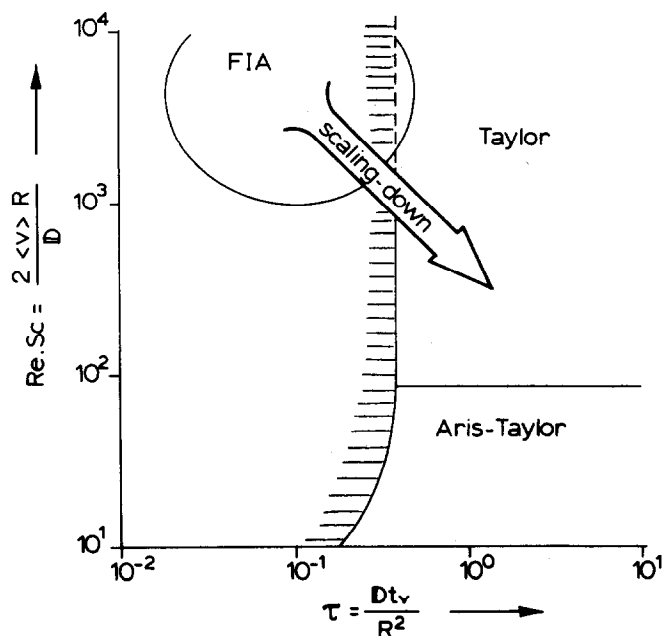


Fig. 3. Graph indicating various flow regions.

the left hand side only numerical results have been presented. The work by Vanderslice *et al.*⁶ needs a special mention here.

Consequence of scaling down

The set of equations on which the further discussion on miniaturisation will be based is summarized in Table I. Additional equations are those for the pressure drop (ΔP) across the tube of length L , and the maximum sampling frequency (expressed in samples per hour). This expression is based on the supposition that two subsequent peaks should be 6σ apart, where σ is expressed in seconds.

The effect of scaling-down, *i.e.* reduction of tube radius, will depend on the restricting conditions imposed on the system⁷. If, for instance, the following

TABLE I. Set of equations on which discussion of miniaturisation is based.

$\Delta P = \frac{8\eta \langle v \rangle L}{R^2}$	$V_R = \pi R^2 L$
$t_v = \frac{L}{\langle v \rangle}$	$f_v = \langle v \rangle \pi R^2$
$\tau = \frac{D t_v}{R^2}$	$\sigma_v = f_v \sigma_t$
$Re \cdot Sc = \frac{2 \langle v \rangle R}{D}$	$f_{\max} = \frac{600}{\sigma_t}$
$\sigma_t = \sqrt{\frac{t_v R^2}{24 D}}$	

conditions are adopted: (1) the residence time remains constant in order to maintain the same degree of conversion in the case of a chemical reaction, and (2) the pressure drop across the conduit does not increase to avoid problems with the pump and the tightness of the connections, then the following influence on the parameters can be expected. A p -fold decrease in tube radius should be accompanied by a decrease of the product $\langle v \rangle L$ with a factor p^2 in order to keep the pressure drop constant. Because $t_v = L/\langle v \rangle$ is assumed to be constant, this means that both L and $\langle v \rangle$ have to decrease by a factor p . This results in a reduction of both $Re \cdot Sc$ and τ by p^2 . This means that the region of operation shifts in the direction indicated by the arrow in Fig. 3.

The advantage is that the flow conditions will become more 'Taylor-like', resulting in more symmetrical peaks. A disadvantage is that the tube volume (V_R) decreases by a factor p^3 and that the injected volume has to be diminished accordingly. This may lead to technical difficulties. An even greater problem, however, is the decrease of σ_v by a factor p^4 . The maximum allowable detector volume is defined by σ_v and here the analyst will very quickly run into difficulties because of lack of suitable detectors.

Another approach in discussing the effect of scaling is to introduce some constraints and to evaluate the segment in a L versus $\langle v \rangle$ graph where the constraints are not surpassed.

In Figs. 4 and 5 the results are shown for two different tube radii. The indicated constraints are:

- $\tau \geq 1$. This means Taylor-flow. The corresponding relation is

$$L \geq \frac{R^2}{D \langle v \rangle}$$

- $f_{\max} \geq 60 \text{ h}^{-1}$. This means a minimum sampling frequency of one sample per minute. The corresponding relation is

$$L \leq \left(\frac{600}{f_{\max}} \right)^2 \frac{24 D \langle v \rangle}{R^2}$$

- $\Delta P \leq \Delta P_{\max} (= 5 \cdot 10^4 \text{ Pa})$. This corresponds to a maximum pressure drop across the conduit of 0.5 bar. The corresponding relation is

$$L \leq \frac{\Delta P_{\max} R^2}{8\eta} \cdot \frac{1}{\langle v \rangle}$$

- $V_{\text{det}} \geq \dots \mu\text{l}$. This means that the detector volume corresponds to the value indicated. The relation used is

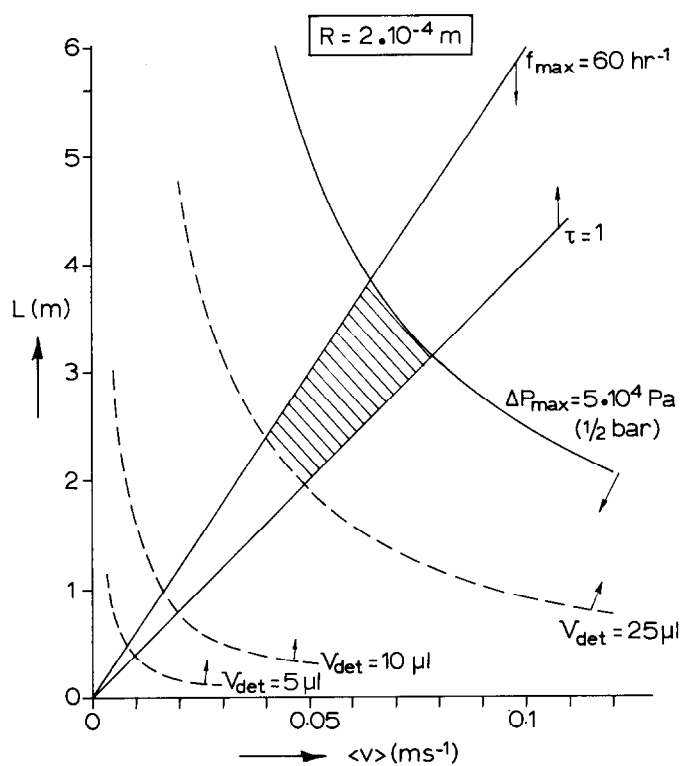


Fig. 4. Graph showing the constraints discussed in the text. The enclosed shaded area indicates the possible L - $\langle v \rangle$ pairs for which $f_{\max} \geq 60 \text{ h}^{-1}$; $\tau > 1$; $V_{\text{det}} \geq 25 \mu\text{l}$ and $\Delta P \leq 1/2 \text{ bar}$. The tube radius is 0.2 mm . $D = 10^{-9} \text{ m}^2 \text{ s}^{-1}$.

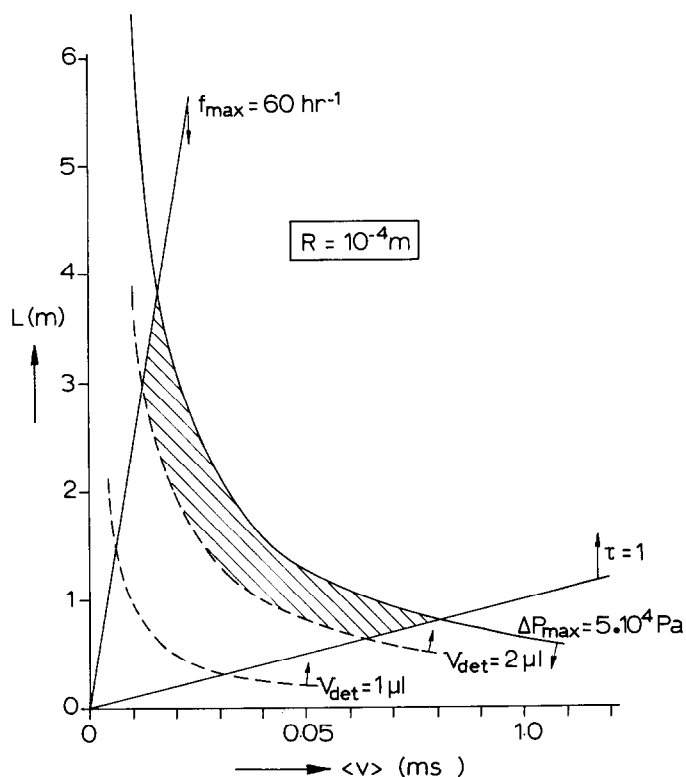


Fig. 5. Graphs as in Fig. 4, but with a tube radius of 0.1 mm .

$$L \geq \frac{96D V_{\text{det}}^2}{\pi^2 R^6} \cdot \frac{1}{\langle v \rangle}$$

Here V_{det} is taken equal to $1/2 \sigma_V$.

In Fig. 4 the shaded area shows the region in which the combinations of L and $\langle v \rangle$ values are located within the constraints. A reduction of the tube radius by a factor of two already shows a dramatic change (Fig. 5). The slope of the f_{\max} line strongly increases whereas the slope of the τ line decreases. This would suggest a much broader choice of suitable L and $\langle v \rangle$ values if the lines for ΔP and V_{det} would not change their position. However, this is not the case. On decreasing R the ΔP line shifts in the direction of the origin while at the same time the V_{det} line shifts in the opposite direction. As can be seen it will be especially the latter value that will set technical limits on possible miniaturisation efforts because detector volumes well below $1 \mu\text{l}$ should be available for a price that must be reasonable in comparison to the other components in FIA manifolds. Possible candidates will be microelectrodes and their optical equivalents: the optrodes.

In conclusion it can be stated that the smallest tube radius of about 0.2 mm used in FIA nowadays is close to the theoretical limit dictated by the available detectors. It is useless to pursue further miniaturisation as long as no suitable sub-microliter detectors are available.

References

- 1 J. B. Angell, S. C. Terry and P. W. Barth, *Sci. Am.*, 248 (1983) 36.
- 2 J. Růžička, *Anal. Chem.*, 55 (1983) 1040 A.
- 3 J. Růžička and E. H. Hansen, *Anal. Chim. Acta*, 161 (1984) 1.
- 4 G. Taylor, *Proc. R. Soc. London, Ser. A*, 219 (1953) 186.
- 5 V. Ananthakrishnan, W. N. Gill and A. J. Barduhn, *AIChE J.*, 11 (1965) 1063.
- 6 J. T. Vanderslice, A. G. Rosenfeld and G. R. Beecher, *Anal. Chim. Acta*, 179 (1986) 119.
- 7 W. E. van der Linden, *Anal. Chim. Acta*, 180 (1986) 20.

W. E. van der Linden is at the Laboratory for Chemical Analysis, Department of Chemical Technology, University of Twente, P.O. Box 217, 7500 AE Enschede, The Netherlands.